Self-Assembly

DOI: 10.1002/anie.201309374

Lability-Controlled Syntheses of Heterometallic Clusters**

*Graham N. Newton, Kiyotaka Mitsumoto, Rong-Jia Wei, Fumichika Iijima, Takuya Shiga, Hiroyuki Nishikawa, and Hiroki Oshio**

Abstract: *A bulky bidentate ligand was used to stabilize a macrocyclic $[Fe^{III}_8Co^{II}_6]$ cluster. Tuning the basicity of the ligand by derivatization with one or two methoxy groups led to the isolation of a homologous $[Fe^{III}_8Co^{II}_6]$ species and a $[Fe^{III}_6Fe^{II}_2Co^{III}_2Co^{II}_2]$ complex, respectively. Lowering the reaction temperatures allowed isolation of $[Fe^{III}_6Fe^{II}_2Co^{III}_2Co^{II}_2]$ clusters with all three ligands. Temperature-dependent absorption data and corresponding experiments with iron/nickel systems indicated that the iron/cobalt self-assembly process was directed by the occurrence of solution-state electron-transfer-coupled spin transition (ETCST) and its influence on reaction intermediate lability.*

Cyanometalate coordination chemistry has led to the development of many heterometallic Prussian Blue analogues (PBAs); 3D arrays that have been shown to display extraordinary physical properties including high-temperature magnetism, electrochromism, and photomagnetism.[1] In recent years, however, molecular systems reminiscent of PBA building blocks have been synthesized in a wide range of shapes and sizes,[2] from dimers,[3] squares,[4] trigonal pyramids[5] and cubes,[6] to larger clusters[7] and infinite 1D chains.[8] Such systems have displayed physical properties with potential applications in future technologies, such as single-molecule magnetism,[9] multi-stable redox behavior,[10] and thermal and photo-induced magnetic bistability.[11]

Heterometallic cyanide-bridged {FeCo} systems have shown thermal and photo-induced magnetic switching through electron-transfer-coupled spin transition (ETCST). First reported in a PBA by Hashimoto and co-workers,[12] the photo-induced phenomenon follows a multistep pathway; firstly electron transfer occurs between the heterometallic centers, converting the low-temperature diamagnetic phase $[(LS\text{-}Fe^{II})(LS\text{-}Co^{III})]$, termed LT, to an intermediate $[(LS\text{-}Fe^{III})(LS\text{-}Co^{II})]$ state, before the Co^{II} ion undergoes spin transition (LS to HS; HS and LS are high-spin and low-spin, respectively) to reach a metastable paramagnetic excited state, $[(LS\text{-}Fe^{III})(HS\text{-}Co^{II})]$, termed HT*). The low temperatures at which the HT* phase is accessed allow it to display single molecule magnet (SMM) or single chain magnet (SCM) type properties.[13] Thermal ETCST can occur at ambient temperatures, where warming can induce LT to HT (high-temperature paramagnetic phase) transition. We recently showed that this behavior can be accompanied by dielectric relaxation and insulator to semiconductor transition in a 1D cyanide-bridged chain.[14]

Their rich functionality and modular synthesis make heterometallic cyanide-bridged complexes attractive targets. We previously reported the synthesis and physical properties of an ETCST-active cyanide-bridged [FeCo] cluster, $[Fe_8Co_6(CN)_{24}(tp)_8(HL1)_{10}(CH_3CN)_2][PF_6]_4{\cdot}14\,CH_3CN{\cdot}5\,H_2O$ (**1a**·14 CH_3CN·5 H_2O),[15] (HL1 = 3-(2-pyridyl)-5-[4-(diphenylamino)phenyl]-1H-pyrazole; tp^- = hydrotris(pyrazolylborate)), in which hydrogen-bond donors and bulky triphenylamine (TPA) units stabilized a 14-metal macrocycle. We have since found ligand and temperature modification to allow access to different clusters, the assembly of which can be understood in terms of the labilities of their reaction intermediates. We herein report the lability-controlled syntheses of heterometallic clusters, in which the lability and electronic states were tuned by ETCST.

The bidentate ligand HL1 was prepared by Claisen condensation of acetyl-substituted TPA and pyridyl carboxylate ethyl ester, followed by dehydration of the β-diketone with hydrazine,[15] as were the mono- and dimethoxy substituted derivatives, HL2 and HL3, respectively (Figure 1, and in the Supporting Information Scheme S1). Cyclic voltammetry (CV) measurements on HL1 (Figure 1), showed one quasi-reversible wave, centered at $E° = 0.90$ V vs. SCE (TPA oxidation to cation radical).[16] Measurements of HL2 and HL3 showed the wave to shift to $E° = 0.76$ and 0.65 vs. SCE, respectively, as a result of electron donation from the methoxy substituents. Changes to the basicity of the capping

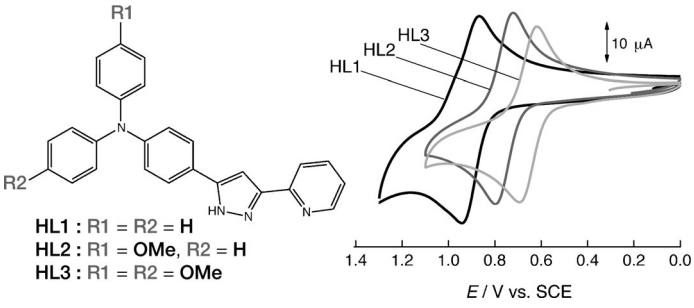

Figure 1. The structural formula and cyclic voltammograms (vs. saturated calomel electrode (SCE)) of HL1, HL2, and HL3.

[*] Dr. G. N. Newton, Dr. K. Mitsumoto, R.-J. Wei, F. Iijima, Dr. T. Shiga, Prof. Dr. H. Oshio
Graduate School of Pure and Applied Sciences
University of Tsukuba
Tennodai 1-1-1, Tsukuba 305-8571 (Japan)
E-mail: oshio@chem.tsukuba.ac.jp
Prof. Dr. H. Nishikawa
Department of Chemistry, Faculty of Science, Ibaraki University
2-1-1 Bunkyo, Mito, Ibaraki 310-8371 (Japan)

[**] This work was supported by a Grant-in-Aid for Scientific Research and for Priority Area "Coordination Programming" (area 2107) from MEXT (Japan), and the JSPS. R.J.W. thanks the China Scholarship Council for funding.

Supporting information for this article is available on the WWW under http://dx.doi.org/10.1002/anie.201309374.

ligands in ETCST-active systems have direct effects on the redox properties and electronic states of the complexes.[11] The ETCST phenomenon can thus be used as a directing tool in the synthesis of mixed-metal clusters.

Complexes were prepared by the synthetic approach employed to isolate red crystals of **1a**;[15] the mixing of HL1, $Co(BF_4)_2{\cdot}6H_2O$, $nBu_4N[Fe(CN)_3(tp)]$, and nBu_4NPF_6 in MeCN, and subsequent slow evaporation or propanol diffusion. Using HL2 in place of HL1 yielded red crystals of $[Fe_8Co_6(CN)_{24}(tp)_8(HL2)_{10}(CH_3CN)_2][PF_6]_4{\cdot}42\,MeCN{\cdot}25\,H_2O{\cdot}9\,iPr_2O$ (**2a**·42 MeCN·25 H_2O·9 iPr_2O),[17] a macrocyclic cluster homologous to **1a**. In contrast, use of HL3 gave green crystals of $[Fe_8Co_4(CN)_{24}(tp)_8(HL3)_6]{\cdot}8\,MeCN{\cdot}28\,H_2O$ (**3**·8 MeCN·28 H_2O), a dodecanuclear cluster (Figure S1). Corresponding control reactions with $Ni(BF_4)_2{\cdot}6H_2O$ in place of cobalt gave three further homologues of **1a**: $[Fe_8Ni_6(CN)_{24}(tp)_8(L)_{10}(CH_3CN)_2][PF_6]_4$. (L = HL1, **4**;[15] HL2, **5**; HL3, **6**, see Supporting Information, Figure S2 and S3). Complexes **1b** and **2b**, with the same core as **3**, were isolated when reactions with HL1 and HL2 were performed at −18 °C. Temperature variations in the syntheses of **3**, and controls **4**, **5**, and **6**, had no perceivable effect on the product in the range tested.

Complex **2a** crystallized in the monoclinic space group $P2_1/c$, with a structure almost identical to **1a** (Figure S1).[15] Bond lengths and magnetic data (Figure S4) suggest the cluster contains eight LS-Fe^{III} and six HS-Co^{II} ions, abbreviated as $[(LS\text{-}Fe^{III})_8(HS\text{-}Co^{II})_6]$. The ion $\mathbf{2a}^{4+}$ has a twelve-membered cyanide-bridged crown core structure, in which Fe^{III} and Co^{II} ions are alternately arranged, with two pendant Fe^{III} ions. The Co^{II}–N bond lengths are in the range 2.026(5)–2.171(6) Å at 100 K; characteristic of HS-Co^{II} ions. The Fe–C bond lengths are in the range 1.849(7)–2.040(6) Å and the Fe–N–C bonds are close to linear, with angles of 164.7(7)–177.7(7)°. Note that LS-Fe^{II} and LS-Fe^{III} centers are usually indistinguishable by bond lengths alone, but their electronic states can be accurately determined from their Mössbauer spectra.[18]

Complex **3** crystallized on an inversion center in the triclinic space group $P\bar{1}$, with a dodecanuclear core composed of eight iron and four Co ions, in which a $\{Fe_2Co_2\}$ molecular square is linked to two tetranuclear $\{Fe_3Co\}$ complexes by cyanide bridges (Figure S1). The bond lengths around the Co ions in the square and tetranuclear $\{Fe_3Co\}$ units are in the range 1.858(10)–1.958(6) and 2.063(9)–2.282(8) Å, indicative of LS-Co^{III} and HS-Co^{II} ions, respectively. The average bond lengths around the iron ions in the square and peripheral iron ions are very similar, at 1.952(10) and 1.947(11) Å, respectively, but their oxidation states are different. Charge balance, magnetic data, and Mössbauer analyses (Figure S4 and S7, Table S2) suggested that the iron ions in the square were LS-Fe^{II} ions and the others were in the LS-Fe^{III} state, giving a formula of $[(LS\text{-}Fe^{III})_6(LS\text{-}Fe^{II})_2(LS\text{-}Co^{III})_2(HS\text{-}Co^{II})_2]$.

Magnetic susceptibility data (Figure S2) supported the compositional assignments of **1a**, **2a**, and **3**, and revealed all fresh samples exhibit antiferromagnetic coupling.

The different cluster topologies obtained from the reactions of cobalt with HL1/HL2 and HL3 were accessed under identical experimental conditions, prompting us to consider the role of the ligand derivatization in the self-assembly process. Although the addition of methoxy groups increased the steric bulk of the ligands, there was no crystallographic evidence that dimethoxy substitution (HL3) would preclude the formation of clusters of type **1a** and **2a**. The key structure-directing factor was likely to be the oxidation-state-driven lability of the cobalt ions; in turn governed by the ligand basicity. The redox potentials of HL1, HL2, and HL3 were 0.90, 0.76, 0.65 V, respectively, and the negatively shifted oxidation potential shows methoxy derivatization to progressively increase the ligand basicity, thus stabilizing trivalent cobalt ions. A clue to the self-assembly process is given by the square $\{Fe_2Co_2\}$ core structure of complex **3**. The combination of bidentate ligands with transition-metal salts and tricyanometalates is a common approach to the synthesis of molecular squares.[4] With this in mind, a reaction scheme is proposed by which all three reactions can proceed through an intermediate square species (Figure 2). Mixtures of bidentate ligands with $Co(BF_4)_2{\cdot}6H_2O$ and $nBu_4N[Fe(CN)_3(tp)]$ form squares that have either diamagnetic $[(LS\text{-}Fe^{II})_2(LS\text{-}Co^{III})_2]$ or paramagnetic $[(LS\text{-}Fe^{III})_2(HS\text{-}Co^{II})_2]$ states.[4] Using HL1 and HL2, cobalt is likely to be stabilized in the Co^{II} (HS) state, generating a labile $[(LS\text{-}Fe^{III})_2(HS\text{-}Co^{II})_2]$ intermediate. With HL3, however, the increased ligand basicity will encourage solution-state ETCST within the intermediate, pushing the equilibrium towards retention of the diamagnetic core ($[(LS\text{-}Fe^{II})_2(LS\text{-}Co^{III})_2]$). To investigate the mechanism, the syntheses of **1a** and **2a** were repeated at −18 °C to trap the ETCST-directed diamagnetic products. Whereas **1a** and **2a** were isolated as red crystals at 25 °C, reactions at −18 °C yielded

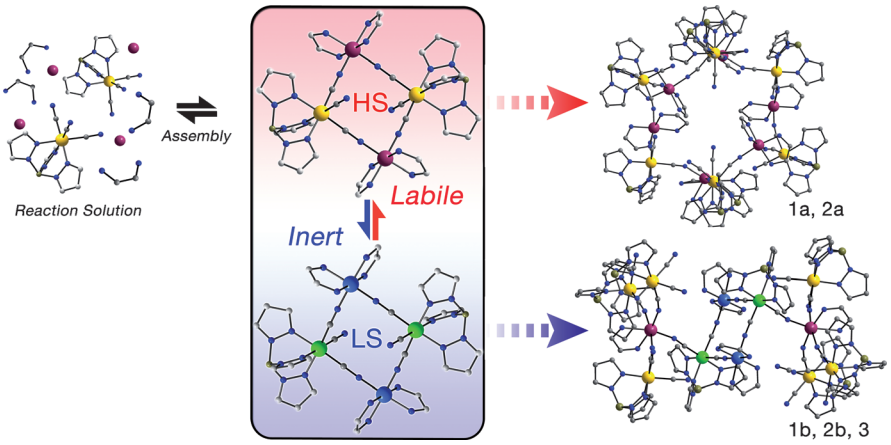

Figure 2. Proposed reaction mechanism of the self-assembly of **1a**, **1b**, **2a**, **2b**, and **3**. Cobalt capping ligands are simplified to bidentate ligands. Metals large spheres, non-metals small spheres: LS-Fe^{III} gold, LS-Co^{III} blue, LS-Fe^{II} green, HS-Co^{II} purple, C gray, N blue, O red.

green crystals of $[Fe_8Co_4(CN)_{24}(tp)_8(HL1)_6]\cdot 10\,MeCN\cdot 4\,H_2O$ (**1b**·10 MeCN·4 H_2O) and $[Fe_8Co_4(CN)_{24}(tp)_8(HL2)_6]\cdot 19\,MeCN\cdot 14\,H_2O$ (**2b**·19 MeCN·14 H_2O), structurally and electronically characterized as homologues of **3** (Figure S7–S9).

Temperature-controlled UV/Vis measurements were conducted on butyronitrile solutions of crystalline samples of **1a**, **1b**, **2a**, **2b**, and **3** to investigate the solution stability of the intact clusters (Figure S10). Data collected at 20 °C for all the samples showed a peak centered around 625 nm, corresponding to the $Co^{II}\rightarrow Fe^{III}$ intervalence charge-transfer (IVCT) transition, while **1b**, **2a**, **2b**, and **3** had a second broad absorption around 750 nm corresponding to the $Fe^{II}\rightarrow Co^{III}$ IVCT band.[11] The spectra of **1b**, **2b**, and **3** showed little temperature dependence, suggesting the complexes were stable in solution. In contrast, **1a** and **2a** showed uniform increases in both ligand-based and charge-transfer absorption bands as temperature was decreased, indicating the existence of complex disassociation and ETCST equilibria.

Absorption spectra, were collected between 25 °C and −60 °C, for reaction solutions (1 mL of acetonitrile reaction solution diluted with 3 mL butyronitrile to give 0.125 mM complex solution, calculated based on Fe) of **1a**, **2a**, and **3** to investigate the self-assembly equilibria (Figure 3). The **1a** reaction solution showed a $Co^{II}\rightarrow Fe^{III}$ IVCT band, but negligible $Fe^{II}\rightarrow Co^{III}$ IVCT absorbance, in agreement with

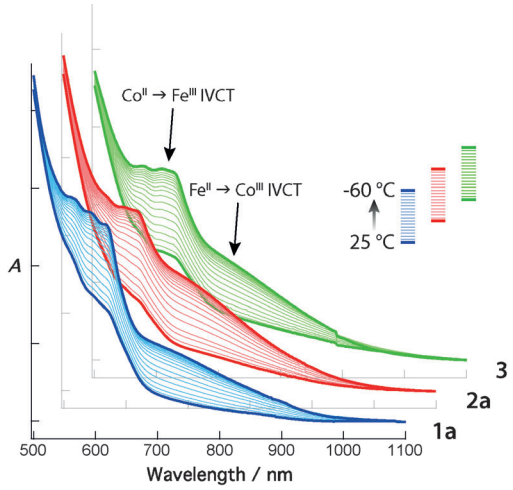

Figure 3. Absorption spectra of reaction solutions (0.125 mM) of **1a** (blue), **2a** (red), and **3** (green), between 25 °C and −60 °C.

the presence of the expected $[(LS\text{-}Fe^{III})_2(HS\text{-}Co^{II})_2]$ species alone. Mirroring the temperature-dependent behavior of the solution of crystalline sample, an $Fe^{II}\rightarrow Co^{III}$ IVCT absorption band appeared as the temperature was lowered and the equilibrium shifted towards the formation of the less-labile $[(LS\text{-}Fe^{II})_2(LS\text{-}Co^{III})_2]$ species. In contrast, the spectra for the reaction solutions of **2a** and, more prominently, **3**, showed $Fe^{II}\rightarrow Co^{III}$ IVCT bands at 25 °C, the intensity of which increased as the temperature was lowered. It is proposed that complexes **1b**/**2b** and **3** are isolated as a result of solution-state ETCST, driven by temperature and Co^{III}-stabilizing ligand basicity, pushing the self-assembly equilibria towards the formation of the more-inert reaction intermediate. Rewarming the samples caused the absorption spectra to revert to their original profiles. The reversible temperature dependence indicates that cluster formation occurs over a significantly longer time than that studied.

In summary, complexation of cobalt ions with HL1 and tricyanoferrate led to the isolation of a macrocyclic $[Fe_8Co_6]$ cluster (**1a**). Using a monomethoxy derivatized ligand (HL2) led to isolation of a homologous cluster (**2a**), but use of a dimethoxy derivative (HL3) generated a dodecanuclear $[Fe_8Co_4]$ complex (**3**) in which a diamagnetic $[Fe^{II}{}_2Co^{III}{}_2]$ square core was capped by two $[Fe^{III}{}_3Co^{II}]$ units. A mechanism was proposed by which the electron-rich, and therefore Co^{III}-stabilizing, ligand HL3 encouraged the occurrence of solution-state ETCST and allowed the trapping of a relatively inert square reaction intermediate. Subsequent experiments on cooled reaction solutions of **1a** and **2a** led to the isolation of homologous $[Fe_8Co_4]$ clusters, **1b** and **2b**. The results of control experiments with Ni confirmed that the self-assembly was directed by solution-state ETCST. This first example of ETCST-directed heterometallic cluster self-assembly may aid the design of switchable cyanide-bridged molecular systems towards functional molecular devices.

Experimental Section

Synthetic procedures: All solvents and chemicals were reagent-grade, purchased commercially, and used without further purification unless noted. Toluene was distilled from CaH_2. Ligand reactants were prepared following reported methods.[19,20] For ligand syntheses see Supporting Information. Complexes **1a** and **4** were synthesized by the reported procedure.[15]

2a: $Co(BF_4)_2\cdot 6\,H_2O$ (5.4 mg, 0.016 mmol) and HL2 (14.3 mg, 0.032 mmol) were combined in acetonitrile (2 mL). The solution was stirred for 5 min then combined with $n$$Bu_4NPF_6$ (31 mg, 0.08 mmol) and $n$$Bu_4N[Fe(CN)_3(tp)]$ (9.4 mg, 0.016 mmol) in acetonitrile (2 mL). Diisopropylether diffusion gave red crystals of **2a**, yield: 2.43 mg (15 %). Elemental analysis (%) calcd for $C_{370}H_{300}N_{114}B_8Co_6F_{24}Fe_8P_4\cdot 2\,CH_3CN\cdot 23\,H_2O$: C 54.08, H 4.27, N 19.56; found: C 53.74, H 4.04, N 19.85.

3: $Co(BF_4)_2\cdot 6\,H_2O$ (5.4 mg, 0.016 mmol) and HL3 (14.3 mg, 0.032 mmol) were combined in acetonitrile (2 mL). The solution was stirred for 5 min then combined with $n$$Bu_4NPF_6$ (31 mg, 0.08 mmol) and $n$$Bu_4N[Fe(CN)_3(tp)]$ (9.4 mg, 0.016 mmol) in acetonitrile (2 mL). Slow evaporation gave dark green crystals of **3**, yield: 5.8 mg (49 %). Elemental analysis (%) calcd for $C_{264}H_{224}B_8Co_4Fe_8N_{96}O_{12}\cdot 12\,H_2O$: C 53.58, H 4.22, N 22.72; found: C 53.43, H 4.36, N 22.72.

1b: $Co(BF_4)_2\cdot 6\,H_2O$ (5.4 mg, 0.016 mmol) and HL1 (14.3 mg, 0.032 mmol) were combined in acetonitrile (2 mL). The solution was stirred for 5 min then combined with $n$$Bu_4NPF_6$ (31 mg, 0.08 mmol) and $n$$Bu_4N[Fe(CN)_3(tp)]$ (9.4 mg, 0.016 mmol) in acetonitrile (2 mL), and the resultant mixture was stored at −18 °C for two weeks, after which dark green crystals of **1b** were isolated. Yield: 5.1 mg (56 %). Elemental analysis (%) calcd for $C_{252}H_{200}N_{96}B_8Co_4Fe_8\cdot 11\,H_2O$: C 54.63, H 4.04, N 24.27; found: C 54.51, H 3.98, N 24.53.

2b: $Co(BF_4)_2\cdot 6\,H_2O$ (5.4 mg, 0.016 mmol) and HL2 (14.3 mg, 0.032 mmol) were combined in acetonitrile (2 mL). The solution was stirred for 5 min then combined with $n$$Bu_4NPF_6$ (31 mg, 0.08 mmol) and $n$$Bu_4N[Fe(CN)_3(tp)]$ (9.4 mg, 0.016 mmol) in acetonitrile (2 mL), and the resultant mixture was stored at −18 °C for two weeks, after which dark green crystals of **2b** were isolated. Yield: 7.2 mg (49 %).

Elemental analysis (%) calcd for $C_{258}H_{212}B_8Co_4Fe_8N_{96}O_6 \cdot 10H_2O$: C 54.34, H 4.10, N 23.58; found: C 54.50, H 4.22, N 23.59.

Received: October 28, 2013
Revised: January 10, 2014
Published online: February 19, 2014

Keywords: cyanide bridges · ETCST · heterometallic complexes · mixed-valent compounds · self-assembly

[1] a) T. Mallah, S. Thiébaut, M. Verdaguer, P. Veillet, *Science* **1993**, *262*, 1554 – 1557; b) K. Itaya, I. Uchida, V. D. Neff, *Acc. Chem. Res.* **1986**, *19*, 162 – 168; c) S. Ohkoshi, H. Tokoro, T. Matsuda, H. Takahashi, H. Irie, K. Hashimoto, *Angew. Chem.* **2007**, *119*, 3302 – 3305; *Angew. Chem. Int. Ed.* **2007**, *46*, 3238 – 3241; d) H. Tokoro, S. Ohkoshi, K. Hashimoto, *Appl. Phys. Lett.* **2003**, *82*, 1245 – 1247.

[2] M. Shatruk, C. Avendano, K. R. Dunbar, *Prog. Inorg. Chem.* **2009**, *56*, 155 – 334.

[3] L. G. Beauvais, J. R. Long, *J. Am. Chem. Soc.* **2002**, *124*, 2110 – 2111.

[4] G. N. Newton, M. Nihei, H. Oshio, *Eur. J. Inorg. Chem.* **2011**, 3031 – 3042.

[5] K. E. Funck, M. G. Hilfiger, C. P. Berlinguette, M. Shatruk, W. Wernsdorfer, K. R. Dunbar, *Inorg. Chem.* **2009**, *48*, 3438 – 3452.

[6] J. L. Heinrich, P. A. Berseth, J. R. Long, *Chem. Commun.* **1998**, 1231 – 1232.

[7] T. Shiga, G. N. Newton, J. S. Mathieson, T. Tetsuka, M. Nihei, L. Cronin, H. Oshio, *Dalton Trans.* **2010**, *39*, 4730 – 4733.

[8] N. Hoshino, Y. Sekine, M. Nihei, H. Oshio, *Chem. Commun.* **2010**, *46*, 6117 – 6119.

[9] D. Li, S. Parkin, G. Wang, G. T. Yee, A. V. Prosvirin, S. M. Holmes, *Inorg. Chem.* **2005**, *44*, 4903 – 4905.

[10] H. Oshio, H. Onodera, T. Ito, *Chem. Eur. J.* **2003**, *9*, 3946 – 3950.

[11] M. Nihei, Y. Sekine, N. Suganami, K. Nakazawa, A. Nakao, H. Nakao, Y. Murakami, H. Oshio, *J. Am. Chem. Soc.* **2011**, *133*, 3592 – 3600.

[12] O. Sato, T. Iyoda, A. Fujishima, K. Hashimoto, *Science* **1996**, *271 – 274*, 23 – 24.

[13] M. Nihei, Y. Okamoto, Y. Sekine, N. Hoshino, T. Shiga, I. P.-C. Liu, H. Oshio, *Angew. Chem.* **2012**, *124*, 6467 – 6470; *Angew. Chem. Int. Ed.* **2012**, *51*, 6361 – 6364.

[14] N. Hoshino, F. Iijima, G. N. Newton, N. Yoshida, T. Shiga, H. Nojiri, A. Nakao, R. Kumai, Y. Murakami, H. Oshio, *Nat. Chem.* **2012**, *4*, 921 – 926.

[15] K. Mitsumoto, E. Oshiro, H. Nishikawa, T. Shiga, Y. Yamamura, K. Saito, H. Oshio, *Chem. Eur. J.* **2011**, *17*, 9612 – 9618.

[16] E. T. Seo, R. F. Nelson, J. M. Fritsch, L. S. Marcoux, D. W. Leedy, R. N. Adams, *J. Am. Chem. Soc.* **1966**, *88*, 3498 – 3503.

[17] For crystal data see Supporting Information. CCDC 951223 (**1b**), 951224 (**2a**), 951225 (**2b**), 951226 (**3**), 980810 (**5**), and 980811 (**6**) contain the supplementary crystallographic data for this paper. These data can be obtained free of charge from The Cambridge Crystallographic Data Centre via www.ccdc.cam.ac.uk/data_request/cif.

[18] Mössbauer measurements conducted on **2a** at 20 K (Figure S5, Table S1) showed it to contain a mixture of Fe^{III} and Fe^{II} ions in a ratio of 3:1, corresponding to a cluster formula of $\{Fe^{III}{}_6Fe^{II}{}_2Co^{III}{}_2Co^{II}{}_4\}$. Magnetic susceptibility data (Figure S6) subsequently collected on the same sample suggested desolvation inside the Mössbauer spectrometer had caused the sample to exhibit thermal ETCST, explaining the deviation from the expected electronic state. This same desolvation-dependent behavior was observed for cluster **1a**.[15]

[19] H. L. Wang, B. Zhang, W. Y. Xu, Y. Q. Bai, H. Wu, *Acta Crystallogr. Sect. E* **2007**, *63*, o2648 – o2649.

[20] A. A. Kelkar, N. M. Patil, R. V. Chaudhari, *Tetrahedron Lett.* **2002**, *43*, 7143 – 7146.

